Published in final edited form as:
Nat Immunol. 2009 May ; 10(5): . doi:10.1038/ni.1720.

Autophagy enhances the presentation of endogenous viral antigens on MHC class I molecules during HSV-1 infection

Luc English[1], **Magali Chemali**[1], **Johanne Duron**[1], **Christiane Rondeau**[1], **Annie Laplante**[1], **Diane Gingras**[1], **Diane Alexander**[2], **David Leib**[2], **Christopher Norbury**[3], **Roger Lippé**[1], and **Michel Desjardins**[1,4,5]

[1]Département de Pathologie et Biologie Cellulaire, Université de Montréal, Succursale Centre-Ville, Montreal, Quebec, Canada.

[2]Department of Ophthalmology and Visual Sciences, Washington University School of Medicine, St. Louis, Missouri, USA.

[3]Department of Microbiology and Immunology, Pennsylvania State University, Milton S. Hershey College of Medicine, Hershey, Pennsylvania, USA.

[4]Département de microbiologie et immunologie, Université de Montréal, Succursale Centre-Ville, Montreal, Quebec, Canada.

[5]Caprion Pharmaceuticals, Montréal, Québec, Canada.

Abstract

Viral proteins are usually processed by the 'classical' major histocompatibility complex (MHC) class I presentation pathway. Here we showed that although macrophages infected with herpes simplex virus type 1 (HSV-1) initially stimulated $CD8^+$ T cells by this pathway, a second pathway involving a vacuolar compartment was triggered later during infection. Morphological and functional analyses indicated that distinct forms of autophagy facilitated the presentation of HSV-1 antigens on MHC class I molecules. One form of autophagy involved a previously unknown type of autophagosome that originated from the nuclear envelope. Whereas interferon-γ stimulated classical MHC class I presentation, fever-like hyperthermia and the pyrogenic cytokine interleukin 1β activated autophagy and the vacuolar processing of viral peptides. Viral peptides in autophagosomes were further processed by the proteasome, which suggests a complex interaction between the vacuolar and MHC class I presentation pathways.

The elaboration of an efficient immune response against pathogens involves complex intracellular antigen-processing events. Endogenous antigens such as viral proteins synthesized by infected host cells are degraded in the cytoplasm by the proteasome, and the

Correspondence should be addressed to M.D. (michel.desjardins@umontreal.ca).

AUTHOR CONTRIBUTIONS

L.E. planned and did most of the experiments and actively participated in writing the manuscript; M.C. did the experiments with mouse embryonic fibroblasts; J.D. maintained viral stocks; C.R. did the technical work for Epon electron microscopy; A.L. provided technical assistance for immunoblot analysis and immunofluorescence; D.G. did the immunogold labeling and morphological quantification; D.A. and D.L. produced the ICP34.5 HSV-1 mutant; C.N. participated in the planning and development of the antigen-presentation assay and provided help in writing the manuscript; R.L. provided HSV-1 virus stocks and expertise with the infection system and helped write the manuscript; and M.D. planned and directed the work and wrote the manuscript.

Note: Supplementary information is available on the Nature Immunology website.

COMPETING INTERESTS STATEMENT

The authors declare competing financial interests: details accompany the full-text HTML version of the paper at http://www.nature.com/natureimmunology/.

resulting peptides are translocated into the endoplasmic reticulum, where they are loaded onto major histocompatibility complex (MHC) class I molecules. In contrast, exogenous antigens are processed by hydrolases in lytic endovacuolar compartments and are loaded on MHC class II molecules that reach the cell surface using recycling machineries associated with these organelles. Although initially thought to be strictly segregated, these pathways are actually functionally interconnected, as shown by the ability of cells to present exogenous antigens on MHC class I molecules; this process is referred to as 'cross-presentation'[1].

Autophagy, a process that allows the transfer of endogenous cellular components into lytic vacuolar compartments, has been shown to be essential to both innate and adaptive immunity[2–4]. This process can be used to eliminate intracellular bacteria and viruses[5–11]. Furthermore, autophagy can facilitate the presentation of endogenous antigens on MHC class II molecules, thereby leading to activation of $CD4^+$ T cells[12,13]. The nature of the endovacuolar membranes involved in the formation of autophagosomes is still a matter of active investigation, but the endoplasmic reticulum is one potential source of autophagosome membrane[14]. As substantial amounts of viral membrane glycoproteins are synthesized in the endoplasmic reticulum of infected cells, it is likely that some of these antigens will reach lytic vacuolar organelles during autophagy. Despite the fact that several reports have demonstrated that antigens generated in the lumen of phagosomes can be loaded (or 'cross-presented') on MHC class I molecules and trigger a $CD8^+$ T cell response[15–17], it is not known whether a similar process could occur after autophagy. Here we provide evidence that infection of macrophages with herpes simplex virus type 1 (HSV-1) triggered a vacuolar response that increased the presentation of a peptide of HSV-1 glycoprotein B (gB) to $CD8^+$ T cells on MHC class I molecules. This vacuolar response, linked to autophagy, could be modulated by various cytokines and stress conditions.

RESULTS

Two phases of MHC class I presentation

Incubation of BMA3.1A7 (called 'BMA' here) macrophages with HSV-1 expressing a green fluorescent protein (GFP)-tagged capsid protein (K26-GFP) resulted in the infection of about 35% of the cells, as determined by flow cytometry (data not shown). Fluorescence microscopy showed that K26-GFP capsids assembled in the nucleus of infected cells at about 6–8 h after infection, reaching a maximum at about 12 h after infection (data not shown). Starting at 6 h after infection, infected macrophages stimulated a $CD8^+$ T cell hybridoma specific for a peptide of amino acids 498–505 of HSV-1 gB[18,19], as measured by the release of β-galactosidase after T cell activation (**Fig. 1a**). The capacity of macrophages to stimulate $CD8^+$ T cells continued to increase up to 12 h after infection, the time at which cellular mortality induced by the viral infection began to occur (data not shown). This macrophage cell death probably explains the decrease in $CD8^+$ T cell stimulation between 12 h and 14 h after infection (**Fig. 1a**).

Stimulation of the $CD8^+$ T cell hybridoma was much lower after treatment of macrophages with the proteasome inhibitor MG-132 or with brefeldin A, a drug that inhibits the transport of molecules through the biosynthetic pathway (**Fig. 1b**). These results indicate that processing and presentation of the viral antigen gB in infected macrophages involves the 'classical' endogenous pathway of MHC class I presentation. However, bafilomycin A, a drug that inhibits the vacuolar proton pump and the acidification of endosomes and lysosomes, had only a minimal effect during the early period of infection (up to 8 h after infection) but strongly inhibited the capacity of infected macrophages to stimulate $CD8^+$ T cells at 10 h and 12 h after infection (**Fig. 1c**). These results suggest that the initial processing of endogenous gB by the classical pathway is followed by the engagement of a

vacuolar pathway that considerably improves the processing of gB and the activation of $CD8^+$ T cells. The possibility of a contribution by a vacuolar pathway was supported by immunofluorescence analyses that indicated that endogenous gB localized together with the endo-lysosomal marker LAMP-1 during infection (**Fig. 1d**). The possibility of the presence of gB in degradative compartments was further supported by the finding of higher gB expression in infected macrophages treated with bafilomycin (data not shown). These results raised the issue of how gB reaches the lysosomal degradative pathway. The possibility of transfer of gB to lysosomes through phagocytosis of infected cells (cross-presentation) was ruled out by results showing that incubation of $H\text{-}2^b$ BMA macrophages together with HSV-1-infected $H\text{-}2^d$ J774 macrophages did not result in activation of the $H\text{-}2^b$-specific $CD8^+$ T cell hybridoma (**Fig. 1e**). Hence, vacuolar processing of gB in the later period of infection was more likely to involve membrane-trafficking events that occurred exclusively in the infected cell.

Data have shown that endogenous viral proteins can be presented on MHC class II molecules by a process involving autophagy[9], which indicates that trafficking events that enable the transport of endogenous proteins to vacuolar degradative organelles can occur in virus-infected cells. To determine if autophagy was involved in the late processing of endogenous gB and its presentation on MHC class I molecules, we first monitored the presence of LC3, a marker of autophagy, in macrophages at various times after infection (**Fig. 2a**). Although we did not detect it in uninfected cells, we found LC3 beginning at 4–6 h after infection, which indicated that an autophagic response occurred during the late phase of HSV-1 infection in macrophages. Whereas the inhibitory effect of bafilomycin indicated that a vacuolar response of some kind was triggered during the late phase of infection in macrophages (**Fig. 1c**), the possibility of a contribution of autophagy to this process was suggested by the substantial inhibition of the $CD8^+$ T cell–stimulatory capacity of macrophages treated with 3-methyladenine, a commonly used inhibitor of autophagy (**Fig. 2b**). Confirmation of the involvement of autophagy in the processing and presentation of gB peptides on MHC class I molecules was provided by experiments involving small interfering RNA (siRNA)-mediated silencing of Atg5, a protein involved in the formation of autophagosomes[20]. Macrophages treated with a control siRNA had a greater capacity to stimulate $CD8^+$ T cells between 8 h and 12 h after infection, but macrophages treated with Atg5-specific siRNA did not (**Fig. 2c**), which linked this late gain in stimulation to the induction of autophagy.

Further support for the idea that autophagy contributes to the vacuolar processing and presentation of gB on MHC class I molecules was provided by results indicating that treatment of infected macrophages with rapamycin, an inhibitor of the kinase mTOR that stimulates autophagy[21], considerably improved $CD8^+$ T cell stimulation (**Fig. 2d**). We obtained similar results with macrophages exposed to a mild heat shock before infection (39 °C for 12 h), a condition also known to induce autophagy[22] (**Fig. 2d**). The enhanced $CD8^+$ T cell stimulation induced by mTOR or heat shock was abolished by the addition of bafilomycin (**Fig. 2e**). These data further link the vacuolar processing of gB to autophagy. We obtained similar results with mouse embryonic fibroblasts isolated from *Atg5*$^{-/-}$ mice[20] (**Supplementary Fig. 1a** online). Silencing of Atg5 in infected macrophages with siRNA abolished the effect of rapamycin (**Fig. 2f**), which confirmed the specificity of this drug for the autophagic pathway. Similarly, neither bafilomycin (**Supplementary Fig. 1c,d**) nor 3-methyladenine (data not shown) affected the capacity of infected macrophages to stimulate $CD8^+$ T cells when autophagy was inhibited by silencing of Atg5. Our results so far indicated that a vacuolar pathway linked to autophagy, triggered within 8–10 h of infection, enhanced the ability of infected macrophages to stimulate gB-specific $CD8^+$ T cells.

Late-stage autophagy involving the nuclear envelope

To study the autophagic response associated with HSV-1 infection in macrophages, we used immunofluorescence and electron microscopy. We first analyzed the induction of autophagy by assessing the autophagic marker LC3. We noted a weak signal for LC3 in uninfected macrophages (**Fig. 3a**), but uninfected cells submitted to a mild heat shock (**Fig. 3b**) or treated with rapamycin (**Fig. 3c**) had strong punctate LC3 signals in the cytoplasm. In contrast, there was a strong LC3 signal in close association with the nuclear envelope in cells 6–8 h after HSV-1 infection (**Fig. 3d,e**). In many cases, vesicles strongly labeled for LC3 seemed to be connected to the nuclear envelope. The colocalization of LC3 and gB suggested that autophagic structures containing viral proteins might originate in the vicinity of the nucleus at a late phase of infection. The difference between the typical labeling noted when autophagy was triggered by rapamycin and that in infected cells might be linked to the fact that HSV-1 infection has been shown to inhibit macroautophagy[23].

The accumulation of LC3 around the nucleus was possibly associated with a cellular process distinct from classical macroautophagy and induced as a late response to infection. To test that hypothesis, we compared the distribution of gB and LC3 in macrophages infected with wild type HSV-1 and a mutant HSV-1 lacking the ICP34.5 protein (Δ34.5); unlike the wild-type virus, this mutant virus is unable to inhibit macroautophagy. As expected, the Δ34.5 virus failed to express any detectable ICP34.5 protein (data not shown). In addition, consistent with the ability of ICP34.5 to mediate dephosphorylation of the translation-initiation factor eIF2α[24], the Δ34.5 virus induced more phosphorylated eIF2α than did wild-type HSV-1 (data not shown). Macrophages infected with the Δ34.5 virus showed considerable accumulation of LC3 on vesicular structures, which also contained large amounts of gB and were present throughout the cytoplasm (**Fig. 3e**). We found no apparent labeling for LC3 in the vicinity of the nuclear envelope. In contrast, infection with the corresponding wild-type virus (strain 17+) led to the accumulation of LC3 near the nuclear envelope between 6 h and 8 h after infection (**Fig. 3e**); these results are in agreement with results obtained with the KOS wild-type strain (**Fig. 3d**). These findings collectively suggested that distinct types of autophagic structures were induced in response to the Δ34.5 and wild type viruses. Macrophages infected with Δ34.5 or wild-type HSV-1 (at an identical multiplicity of infection) were able to stimulate gB-specific $CD8^+$ T cells to a similar extent (**Fig. 3f**). However, the expression of HSV-1 proteins (**Fig. 3g**) and gB (**Fig. 3h**) was much lower in macrophages infected with the Δ34.5 virus, in agreement with published studies[25,26]. Thus, macrophages infected with the Δ34.5 virus stimulated gB-specific $CD8^+$ T cells much more efficiently. Bafilomycin strongly inhibited the stimulatory ability of macrophages infected with either Δ34.5 or wild-type HSV-1 (**Fig. 3i**), which emphasizes the involvement of a vacuolar pathway in both cases.

To characterize the autophagosomal structures induced during the late phase of infection, we used electron microscopy for detailed morphological analysis (**Fig. 4** and **Supplementary Fig. 2** online). We noted two types of prominent structures in infected cells. The first was characterized by the presence of double-membraned structures reminiscent of the morphology of autophagosomes found in cells treated with rapamycin (**Supplementary Fig. 2a**). These structures often surrounded viral particles in the cytoplasm (**Supplementary Fig. 2b**). The degradation of microbial invaders by autophagy has been described before and is referred to as ‘xenophagy’[27]. These structures showed substantial labeling for LC3 and, to a lesser extent, for gB (**Supplementary Fig. 2c,d**), which confirmed the presence of viral proteins in autophagosomes. The second type of organelle had multiple membranes either connected to the nuclear envelope or present in the cytoplasm (**Fig. 4a,e**). These structures seemed to emerge through a coiling process of the inner and outer nuclear membrane, forming four-layered structures that engulfed part of the nearby cytoplasm (**Fig. 4b,c**). In

several examples, similar structures containing cytoplasm and unenveloped viral capsids seemed to be disconnected from the nucleus (**Fig. 4d**). These structures were not present in uninfected or rapamycin-treated cells (**Supplementary Fig. 2e**). However, there were more two- and four-membraned structures in infected macrophages at the late phase of infection (**Supplementary Fig. 2e,f**). To determine whether the four-layered membrane structures present in the cytoplasm were similar to those that emerged from the nuclear envelope, we used electron microscopy to locate the product of the enzyme glucose-6-phosphatase, a specific marker of the endoplasmic reticulum and nuclear envelope. The results indicated that the product of glucose-6-phosphatase was restricted to the endoplasmic reticulum and nuclear envelope (**Fig. 4e**). The four-layered membrane structures connected to the nuclear envelope, as well as those present in the cytoplasm, were also positive for glucose-6-phosphatase (**Fig. 4f**), which confirmed their origin in the endoplasmic reticulum and/or nuclear envelope.

To determine whether the four-layered membrane structures had features of autophagosomes, we used immunoelectron microscopy to detect the autophagosome marker LC3. We found accumulation of LC3 on membrane structures emerging from the nuclear envelope, as well as on four-layered membrane structures apparently disconnected from the nucleus and present in the cytoplasm (**Fig. 5a,b**). The association between LC3 and the membrane of autophagosomes indicated that our antibody recognized the LC3-II cleaved form of the protein[28]. Quantitative analysis of the immunolabeling for LC3 showed there was an average (± s.e.m.) of 3.03 ± 0.47 gold particles per mm membrane on autophagosomes, compared with 0.15 ± 0.02 and 0.70 ± 0.15 gold particles per mm membrane for the plasma membrane and nuclear membrane, respectively. We also found gB on the membrane of the nuclear envelope (data not shown), as well as on the four-layered membrane structures (**Fig. 5c**). The ability of these structures to fuse with lytic organelles was confirmed by the presence of bovine serum albumin–gold particles, transferred from lysosomes, in these structures (**Fig. 5d**). These data collectively confirm the autophagosomal nature of the four-layered membrane structures originating from the nuclear envelope.

Cytokines engage classical and vacuolar responses

Treatment of macrophages with the proinflammatory cytokine interferon-γ (IFN-γ) stimulates the clearance of mycobacteria by a process involving autophagy[6]. Therefore, we tested whether this cytokine might promote the vacuolar processing of gB and improve the ability of HSV-1-infected macrophages to stimulate $CD8^+$ T cells. As heat treatment of macrophages stimulated autophagy, we also tested the potential effect of the pyrogenic cytokine interleukin 1β (IL-1β). IFN-γ considerably enhanced the ability of HSV-1-infected macrophages to stimulate $CD8^+$ T cells (**Fig. 6a**). IL-1β and mild heat-shock treatment also augmented the stimulatory capacity of macrophages (**Fig. 6a**). Notably, staining with dansylcadaverin, a marker of autophagy, was greater after exposure to mild heat shock or IL-1β but not after treatment with IFN-γ (**Fig. 6b**). Electron microscopy also showed that cells stimulated with heat shock or IL-1β had more autophagosomes (data not shown). These results suggest that the enhanced ability of macrophages to stimulate $CD8^+$ T cells after treatment with mild heat shock or IL-1β was linked to the contribution of a vacuolar pathway related to autophagy. We confirmed that hypothesis by showing that treatment of IL-1β- or heat shock–treated macrophages with either 3-methyladenine, the inhibitor of autophagy, or bafilomycin, the inhibitor of the vacuolar proton pump, resulted in a much lower capacity of macrophages to stimulate $CD8^+$ T cells than that of control cells (**Fig. 6c–e**). In contrast, the very strong stimulation of $CD8^+$ T cells induced by infected macrophages kept at 37 °C or treated with IFN-γ was not strongly affected by 3-methyladenine or bafilomycin and therefore was not due to vacuolar processing (**Fig. 6c,f**). Confirmation that autophagy did not contribute to the stimulatory effect of IFN-γ was provided by experiments

showing that this cytokine enhanced the capacity of infected embryonic fibroblasts isolated from wild-type and *Atg5*$^{-/-}$ mice to stimulate CD8^{+} T cells (**Supplementary Fig. 2a**). However, the stimulatory effect induced by IL-1β and mild heat shock was completely abolished by brefeldin A and MG-132 (**Fig. 6d,e**). The effect of these two inhibitors of the 'classical' pathway of MHC class I presentation indicated a close interaction occurring between this pathway and the vacuolar pathway in the processing of gB (**Supplementary Fig. 3** online).

DISCUSSION

One of the main components of the complex cell-entry 'machinery' of herpes viruses is gB[29]. This transmembrane protein of the viral envelope is synthesized in the endoplasmic reticulum of infected cells. In agreement with published work[18], we found that gB was expressed within 2 h after infection in BMA macrophages and was present in the perinuclear region of infected cells. gB can also accumulate in the inner membrane as well as the outer membrane of the nuclear envelope[30,31]. Our results indicated that the processing of gB by infected macrophages has two distinct phases. During the first phase, which occurs 6–8 h after infection, gB is processed mainly by the classical pathway of MHC class I presentation, which involves proteasome-mediated degradation and transport steps through the biosynthetic apparatus. During the second phase of infection, which occurs 8–12 h after infection, a vacuolar pathway is triggered and contributes substantially to the capacity of infected macrophages to stimulate CD8^{+} T cells. The cellular trafficking events that enable the transport of gB in the lysosomal degradative pathway are poorly understood. We were able to rule out the possibility of a contribution by a cross-presentation pathway involving the phagocytosis of infected cells by neighboring macrophages, which emphasized the fact that gB reaches the vacuolar processing pathway by an endogenous route. Instead, our results indicated the involvement of autophagy in facilitating the processing and presentation of endogenous viral peptides on MHC class I molecules.

Our findings may seem to contradict earlier reports indicating that HSV-1 inhibits macroautophagy[23]; this inhibition is key to the neurovirulence of the virus[11]. However, a closer look at infected macrophages suggests that a form of autophagy distinct from macroautophagy is triggered. Macroautophagy can be induced in a variety of cells by mild heat shock or treatment with the mTOR inhibitor rapamycin[21,22]. In uninfected macrophages, these conditions induced throughout the cytoplasm the formation of autophagosomes with a double-membraned structure. In contrast, HSV-1-infected macrophages had two types of structures. In addition to the double-membraned structures, four-layered membrane structures that emerged from the nuclear envelope and accumulated in the cytoplasm at around 8 h after infection were present in most infected macrophages. We did not find such structures in uninfected cells treated with rapamycin, which suggested that they arose from a specific host response to HSV-1 infection distinct from macroautophagy. Although four-layered membrane structures have been reported before in the cytoplasm of HSV-1-infected mouse embryonic fibroblasts[25], the autophagosomal nature of those structures was not documented. Here we have shown that these four-layered membrane structures were 'decorated' with LC3, a protein that is key to the formation of autophagosomes[28], and that these structures fused with lysosomes filled with bovine serum albumin–gold, thereby generating an environment suitable for the hydrolytic degradation of gB.

We conclude that the ability of HSV-1 to inhibit macroautophagy early after infection, and thus to potentially limit the presentation of viral peptides, is counterbalanced by a host response involving the induction of a previously unknown autophagy pathway at a later time after infection. Our conclusion is supported by the results obtained with the Δ34.5 mutant

virus. Macrophages infected with this mutant were able to trigger a strong immune response, like macrophages infected with wild-type viruses. Although the apparent magnitude of activation of $CD8^+$ T cells induced by wild-type and Δ34.5 viruses was similar, the quantity of gB and viral proteins expressed in Δ34.5-infected cells was much lower than that in macrophages infected with wild-type HSV-1. Macrophages infected with either Δ34.5 or wild-type HSV-1 engaged strong vacuolar responses. The distinct localization of LC3 to autophagosomes in the cytoplasm in macrophages infected with Δ34.5 virus, in contrast to its localization to the nuclear membrane in macrophages infected with wild-type virus, indicates that both types of autophagic responses can participate in the processing of viral proteins for presentation on MHC class I molecules.

It has been reported that IFN-γ stimulates autophagy and the clearance of mycobacteria in macrophages[3]. In our studies, IFN-γ had no substantial effect on the induction of autophagy, a discrepancy that might be explained by the cell type and/or concentration of the cytokine used for stimulation[32]. Nevertheless, IFN-γ-treated macrophages were much more efficient at stimulating $CD8^+$ T cells after HSV-1 infection. As cotreatment with bafilomycin or 3-methyladenine had no effect on this IFN-γ-induced stimulatory capacity, we conclude that vacuolar processing and autophagy were not essential to the response induced by IFN-γ. The stimulatory effect of IFN-γ on antigen presentation is well established. This cytokine upregulates assembly of the immunoproteasome[33] and stimulates expression of TAP1, the transporter associated with antigen presentation[34], two key components of the classical MHC class I presentation pathway. Therefore, it was not unexpected to find strong inhibition of the stimulation of $CD8^+$ T cells when we treated IFN-γ-stimulated macrophages with MG-132 and BFA. In contrast, the IL-1β-induced improvement in the ability of infected macrophages to stimulate $CD8^+$ T cells was inhibited considerably by 3-methyladenine and bafilomycin, which confirmed the contribution of autophagy to this process.

The similarity in the results obtained with IL-1β and mild heat-shock treatment suggests that IL-1β induces a cellular response similar to the one that occurs during fever-like conditions. Indeed, IL-1β is well known for its ability to induce fever[35]. Tumor necrosis factor, a second pyrogenic cytokine, also stimulated autophagy and the vacuo-lar processing of gB in our system (data not shown). These results suggest that the stress induced during fever conditions or after stimulation with pyrogenic cytokines triggers defense mechanisms, promoting more-efficient processing of viral antigens in vacuolar organelles. Notably, cytomegalovirus, a member of the herpesviridae family, can block signaling by IL-1β and tumor necrosis factor during the early phase of infection[36], a process that might protect the virus by inhibiting the induction of antigen processing through a vacuolar response.

Our results showing that lytic organelles associated with the processing of antigens for presentation on MHC class II molecules[12] participated in the presentation of endogenous viral peptides on MHC class I molecules emphasize the dynamic cooperation between the ‘classical’ and ‘vacuolar’ pathways of antigen presentation. This close interaction is further emphasized by results showing that even in conditions in which vacuolar processing contributes to most of the viral antigen processing, such as after IL-1β or heat-shock stimulation, MG-132 and BFA still had a strong inhibitory effect. These results support a model in which the vacuolar processing of viral proteins in autophagosomes is followed by processing by the proteasome and peptide loading onto MHC class I molecules in the endoplasmic reticulum. The molecular mechanisms that enable the transfer of viral peptides from autophagosomes to proteasomes in the cytoplasm are unknown. A similar transport step has been shown to take place on phagosomes[37]. Although the molecular ‘machines’ that enable these translocation events have not been identified, it has been proposed that endoplasmic reticulum translocons such as Sec61 and/or derlin-1 could be involved[16,17,38].

Although the nature of the endomembranes involved in the formation of autophagosomes during macroautophagy is still a matter of debate, our results have shown that the nuclear envelope, made of endoplasmic reticulum, is the membrane used to form the gB-enriched autophagosomes with four-layered membranes in HSV-1-infected macrophages. The endoplasmic reticulum has been shown to participate in a form of autophagy in yeasts referred to as 'ER-phagy'[14]. Whether this process is homologous with the nuclear envelope–derived autophagic process documented here remains to be investigated. Published studies have shown that viruses take advantage of macroautophagy to find refuge in organelles, where they freely assemble[39]. Our results indicate that autophagy can also benefit the host by providing an additional pathway for the degradation of endogenous viral proteins for antigen presentation.

METHODS

Cells, viruses, antibodies and reagents

The BMA3.1A7 macrophage cell line was derived from C57BL/6 mice as described[37] and was cultured in complete DMEM (10% (vol/vol) FCS, penicillin (100 units/ml) and streptomycin (100 μg/ml)). The mouse macrophage cell line J774 was from American Type Culture Collection. The β-galactosidase–inducible HSV gB–specific $CD8^+$ T cell hybridoma HSV-2.3.2E2 (provided by W. Heath, University of Melbourne) was maintained in RPMI-1640 medium supplemented with 5% (vol/vol) FCS, glutamine (2 mM), penicillin (100 units/ml), streptomycin (100 μg/ml), the aminoglycoside G418 (0.5 mg/ml) and hygromycin B (100 μg/ml). The HSV-1 K26-GFP mutant (strain KOS), carrying a GFP-tagged capsid protein VP26, was provided by P. Desai[40]. The ICP34.5-null virus Δ34.5 was constructed by a strategy similar to that used to make the null mutant 17termA[41]. A 3,333–base pair *DpnII* fragment containing the gene encoding ICP34.5 with a nonsense mutation inserted at the sequence encoding the amino acid at position 30 was transfected into Vero cells together with infectious DNA from HSV-1 strain 17 (ref. 25). Individual plaques resulting from this transfection were screened by PCR amplification, followed by screening by *SpeI* digestion. After three rounds of plaque purification, viral stock was generated from which infectious DNA was prepared and 'marker rescue' was done. The ICP34.5-null Δ34.5 virus was characterized by immunoblot analysis for ICP34.5 and phosphorylated eIF2α as described[25]. Primary antibodies used were as follows: rabbit polyclonal antibody to LC3a (anti-LC3a; AP1801a; Abgent), rabbit polyclonal anti-LC3b (AP1802a; Abgent), rabbit polyclonal antibody to cleaved LC3b (AP1806a; Abgent), mouse monoclonal anti-gB (M612449; Fitzgerald), rat anti-LAMP-1 (1D4B; Developmental Studies Hybridoma Bank), rabbit polyclonal anti-Atg5 (NB-110-53818; Novus Biologicals), mouse monoclonal anti-tubulin (B-5-1-2; Sigma) and rabbit polyclonal anti-HSV (RB-1425-A; Neomarkers). The secondary antibodies Alexa Fluor 568–conjugated goat anti-rabbit, Alexa Fluor 633–conjugated goat anti-mouse and Alexa Fluor 488–conjugated goat anti-mouse were from Invitrogen. Brefeldin A, bafilomycin A, MG-132, 3-methyladenine and rapamicyn were from Sigma.

Heat shock, cytokine treatment and infection

For heat-shock treatment, macrophages (1×10^5 cells per well in 24-well plates) were incubated for 12 h at 39 °C, followed by a recovery period of 2 h at 37 °C before infection. The cytokines IL-1β (5 ng/ml; R&D Systems) and IFN-γ (200 U/ml; PBL) were added 18–24 h before infection and were kept in the medium during viral infection. Macrophages were infected by incubation for 30 min with virus at a multiplicity of infection of 10. Cells were then washed and were incubated in fresh medium for a total of 8 h unless indicated otherwise. Drugs were added to the medium from 2 h after infection until the end of

infection at the following concentrations: brefeldin A, 5 μg/ml; bafilomycin A, 0.5 μM; MG-132, 5 μM; 3-methyladenine, 10 mM; and rapamicyn, 10 μg/ml.

$CD8^+$ T cell hybridoma assay

Mock- or HSV-1-infected macrophages (2×10^5) were washed in Dulbecco's PBS and were fixed for 10 min at 23 °C with 1% (wt/vol) paraformadehyde, followed by three washes in complete DMEM. Antigen-presenting cells were then cultured for 12 h at 37 °C together with 4×10^5 HSV-2.3.2E2 cells (the β-galactosidase–inducible, gB-specific $CD8^+$ T cell hybridoma) for analysis of the activation of T cells. Cells were then washed in Dulbecco's PBS and lysed (0.125 M Tris base, 0.01 M cyclohexane diaminotetraacetic acid, 50% (vol/vol) glycerol, 0.025% (vol/vol) Triton X-100 and 0.003 M dithiothreitol, pH 7.8). A β-galactosidase substrate buffer (0.001 M $MgSO_4 \times 7\ H_2O$, 0.01 M KCl, 0.39 M $NaH_2PO_4 \times H_2O$, 0.6 M $Na_2HPO_4 \times 7\ H_2O$, 100 mM 2-mercaptoethanol and 0.15 mM chlorophenol red β-D-galactopyranoside, pH 7.8) was added for 2–4 h at 37 °C. Cleavage of the chromogenic substrate chlorophenol red-β-D-galactopyranoside was quantified in a spectrophotometer as absorbance at 595 nm.

Immunufluorescence and dansylcadaverin labeling

For immunofluorescence analysis, control, treated and/or infected macrophages were fixed and made permeable with a Cytofix/Cytoperm kit according to the manufacturer's recommendations (BD Biosciences). Cells were then incubated for 60 min at 25 °C with anti-LC3, anti-gB or anti-LAMP-1. For analysis of infection with HSV-1 K26-GFP, infected cells were visualized by detection of GFP fluorescence at 488 nm. Cells were analyzed with a confocal laser-scanning microscope (LSM 510Meta Axiovert; Carl Zeiss) or standard Axiophot fluorescent microscope (Zeiss) or by flow cytometry with a FACSCalibur (BD). For labeling with dansylcadaverin (Sigma), macrophages left untreated or exposed to IL-1β, IFN-γ or mild heat shock were infected for 8 h and then stained for 15 min at 37 °C with 50 μM dansylcadaverin. Cells were then washed in Dulbecco's PBS and were lysed in 200 μl lysis buffer (described above). Total fluorescence was quantified with a SpectraMax Gemini electron microscopy spectrophotometer (excitation, 380 nm; emission, 525 nm).

Electron microscopy

For morphological analysis, cells were fixed in 2.5% (vol/vol) glutaraldehyde and were embedded in Epon (Mecalab). Glucose-6-phosphatase was detected by electron microscopy cytochemistry as described[42]. For immunocytochemistry after embedding, cells were fixed in 1% (vol/vol) glutaraldehyde and were embedded at –20 °C in Lowicryl (Canemco). Lowicryl ultrathin sections were incubated overnight with antibodies and were visualized by 60 min of incubation with protein A–gold complex (10 nm). Rabbit anti-LC3 and mouse anti-gB were used at dilution of 1:10.

Analysis with siRNA

Control siRNA (nontargeting; siCONTROL) and siRNA specific for mouse Atg5 (L-064838-00-0005; ON-TARGETplus SMARTpool) were from Dharmacon. Cells were transfected with 100 nM siRNA using the DermaFECT 4 siRNA transfection reagent according to the manufacturer's recommendations (Dharmacon). After 24 h, transfection medium was replaced by complete medium.

Supplementary Material

Refer to Web version on PubMed Central for supplementary material.

Acknowledgments

We thank J. Thibodeau and C. Perreault for critical reading of the manuscript; K. Rock (University of Massachusetts Medical School) for BMA cells; W. Heath (University of Melbourne) for the HSV-2.3.2E2 hybridoma; G. Arthur (University of Manitoba) for the wild-type and *Atg5*$^{-/-}$ mouse embryonic fibroblasts produced by N. Mizushima (Medical and Dental University, Tokyo); P. Desai (Johns Hopkins University) for the HSV-1 K26-GFP mutant; and M. Bendayan for assistance with electron microscopy. Supported by the Canadian Institutes for Health Research (R.L. and M.D.), the Natural Science and Engineering Research Council of Canada (L.E.), Fonds de la Recherche en Santé du Québec (L.E.), the US National Institutes of Health (EY09083) and Research to Prevent Blindness (D.L.)

References

1. Bevan MJ. Cross-priming for a secondary cytotoxic response to minor H antigens with H-2 congenic cells which do not cross-react in the cytotoxic assay. J. Exp. Med. 1976; 143:1283–1288. [PubMed: 1083422]
2. Deretic V. Autophagy in innate and adaptive immunity. Trends Immunol. 2005; 26:523–528. [PubMed: 16099218]
3. Levine B, Deretic V. Unveiling the roles of autophagy in innate and adaptive immunity. Nat. Rev. Immunol. 2007; 7:767–777. [PubMed: 17767194]
4. Schmid D, Munz C. Innate and adaptive immunity through autophagy. Immunity. 2007; 27:11–21. [PubMed: 17663981]
5. Andrade RM, Wessendarp M, Gubbels MJ, Striepen B, Subauste CS. CD40 induces macrophage anti-Toxoplasma gondii activity by triggering autophagy-dependent fusion of pathogen-containing vacuoles and lysosomes. J. Clin. Invest. 2006; 116:2366–2377. [PubMed: 16955139]
6. Gutierrez MG, et al. Autophagy is a defense mechanism inhibiting BCG and Myco-bacterium tuberculosis survival in infected macrophages. Cell. 2004; 119:753–766. [PubMed: 15607973]
7. Ling YM, et al. Vacuolar and plasma membrane stripping and autophagic elimination of Toxoplasma gondii in primed effector macrophages. J. Exp. Med. 2006; 203:2063–2071. [PubMed: 16940170]
8. Nakagawa I, et al. Autophagy defends cells against invading group A Streptococcus. Science. 2004; 306:1037–1040. [PubMed: 15528445]
9. Ogawa M, et al. Escape of intracellular Shigella from autophagy. Science. 2005; 307:727–731. [PubMed: 15576571]
10. Liu Y, et al. Autophagy regulates programmed cell death during the plant innate immune response. Cell. 2005; 121:567–577. [PubMed: 15907470]
11. Orvedahl A, et al. HSV-1 ICP34.5 confers neurovirulence by targeting the Beclin 1 autophagy protein. Cell Host Microbe. 2007; 1:23–35. [PubMed: 18005679]
12. Paludan C, et al. Endogenous MHC class II processing of a viral nuclear antigen after autophagy. Science. 2005; 307:593–596. [PubMed: 15591165]
13. Dengjel J, et al. Autophagy promotes MHC class II presentation of peptides from intracellular source proteins. Proc. Natl. Acad. Sci. USA. 2005; 102:7922–7927. [PubMed: 15894616]
14. Bernales S, Schuck S, Walter P. ER-phagy: selective autophagy of the endoplasmic reticulum. Autophagy. 2007; 3:285–287. [PubMed: 17351330]
15. Ackerman AL, Kyritsis C, Tampe R, Cresswell P. Early phagosomes in dendritic cells form a cellular compartment sufficient for cross presentation of exogenous antigens. Proc. Natl. Acad. Sci. USA. 2003; 100:12889–12894. [PubMed: 14561893]
16. Houde M, et al. Phagosomes are competent organelles for antigen cross-presentation. Nature. 2003; 425:402–406. [PubMed: 14508490]
17. Guermonprez P, et al. ER-phagosome fusion defines an MHC class I cross-presentation compartment in dendritic cells. Nature. 2003; 425:397–402. [PubMed: 14508489]
18. Mueller SN, et al. The early expression of glycoprotein B from herpes simplex virus can be detected by antigen-specific CD8+ T cells. J. Virol. 2003; 77:2445–2451. [PubMed: 12551982]
19. Mueller SN, Jones CM, Smith CM, Heath WR, Carbone FR. Rapid cytotoxic T lymphocyte activation occurs in the draining lymph nodes after cutaneous herpes simplex virus infection as a

result of early antigen presentation and not the presence of virus. J. Exp. Med. 2002; 195:651–656. [PubMed: 11877488]

20. Kuma A, et al. The role of autophagy during the early neonatal starvation period. Nature. 2004; 432:1032–1036. [PubMed: 15525940]
21. Noda T, Ohsumi Y. Tor, a phosphatidylinositol kinase homologue, controls autophagy in yeast. J. Biol. Chem. 1998; 273:3963–3966. [PubMed: 9461583]
22. Komata T, et al. Mild heat shock induces autophagic growth arrest, but not apoptosis in U251-MG and U87-MG human malignant glioma cells. J. Neurooncol. 2004; 68:101–111. [PubMed: 15218946]
23. Talloczy Z, et al. Regulation of starvation- and virus-induced autophagy by the eIF2α kinase signaling pathway. Proc. Natl. Acad. Sci. USA. 2002; 99:190–195. [PubMed: 11756670]
24. He B, Gross M, Roizman B. The $\gamma_1$34.5 protein of herpes simplex virus 1 complexes with protein phosphatase 1α to dephosphorylate the alpha subunit of the eukaryotic translation initiation factor 2 and preclude the shutoff of protein synthesis by double-stranded RNA-activated protein kinase. Proc. Natl. Acad. Sci. USA. 1997; 94:843–848. [PubMed: 9023344]
25. Alexander DE, Ward SL, Mizushima N, Levine B, Leib DA. Analysis of the role of autophagy in replication of herpes simplex virus in cell culture. J. Virol. 2007; 81:12128–12134. [PubMed: 17855538]
26. Talloczy Z, Virgin HW IV. Levine B. PKR-dependent autophagic degradation of herpes simplex virus type 1. Autophagy. 2006; 2:24–29. [PubMed: 16874088]
27. Levine B. Eating oneself and uninvited guests: autophagy-related pathways in cellular defense. Cell. 2005; 120:159–162. [PubMed: 15680321]
28. Kabeya Y, et al. LC3, a mammalian homologue of yeast Apg8p, is localized in autophagosome membranes after processing. EMBO J. 2000; 19:5720–5728. [PubMed: 11060023]
29. Heldwein EE, et al. Crystal structure of glycoprotein B from herpes simplex virus 1. Science. 2006; 313:217–220. [PubMed: 16840698]
30. Stannard LM, Himmelhoch S, Wynchank S. Intra-nuclear localization of two envelope proteins, gB and gD, of herpes simplex virus. Arch. Virol. 1996; 141:505–524. [PubMed: 8645092]
31. Farnsworth A, et al. Herpes simplex virus glycoproteins gB and gH function in fusion between the virion envelope and the outer nuclear membrane. Proc. Natl. Acad. Sci. USA. 2007; 104:10187–10192. [PubMed: 17548810]
32. Khalkhali-Ellis Z, et al. IFN-γ regulation of vacuolar pH, cathepsin D processing and autophagy in mammary epithelial cells. J. Cell. Biochem. 2008; 105:208–218. [PubMed: 18494001]
33. Griffin TA, et al. Immunoproteasome assembly: cooperative incorporation of interferon γ (IFN-γ)-inducible subunits. J. Exp. Med. 1998; 187:97–104. [PubMed: 9419215]
34. Epperson DE, et al. Cytokines increase transporter in antigen processing-1 expression more rapidly than HLA class I expression in endothelial cells. J. Immunol. 1992; 149:3297–3301. [PubMed: 1385520]
35. Conti B, Tabarean I, Andrei C, Bartfai T. Cytokines and fever. Front. Biosci. 2004; 9:1433–1449. [PubMed: 14977558]
36. Jarvis MA, et al. Human cytomegalovirus attenuates interleukin-1b and tumor necrosis factor α proinflammatory signaling by inhibition of NF-kB activation. J. Virol. 2006; 80:5588–5598. [PubMed: 16699040]
37. Kovacsovics-Bankowski M, Rock KL. A phagosome-to-cytosol pathway for exogenous antigens presented on MHC class I molecules. Science. 1995; 267:243–246. [PubMed: 7809629]
38. Ackerman AL, Giodini A, Cresswell P. A role for the endoplasmic reticulum protein retrotranslocation machinery during crosspresentation by dendritic cells. Immunity. 2006; 25:607–617. [PubMed: 17027300]
39. Jackson WT, et al. Subversion of cellular autophagosomal machinery by RNA viruses. PLoS Biol. 2005; 3:e156. [PubMed: 15884975]
40. Desai P, Person S. Incorporation of the green fluorescent protein into the herpes simplex virus type 1 capsid. J. Virol. 1998; 72:7563–7568. [PubMed: 9696854]

41. Bolovan CA, Sawtell NM, Thompson RL. ICP34.5 mutants of herpes simplex virus type 1 strain 17syn+ are attenuated for neurovirulence in mice and for replication in confluent primary mouse embryo cell cultures. J. Virol. 1994; 68:48–55. [PubMed: 8254758]

42. Griffiths G, Quinn P, Warren G. Dissection of the Golgi complex. I. Monensin inhibits the transport of viral membrane proteins from medial to trans Golgi cisternae in baby hamster kidney cells infected with Semliki Forest virus. J. Cell Biol. 1983; 96:835–850. [PubMed: 6682112]

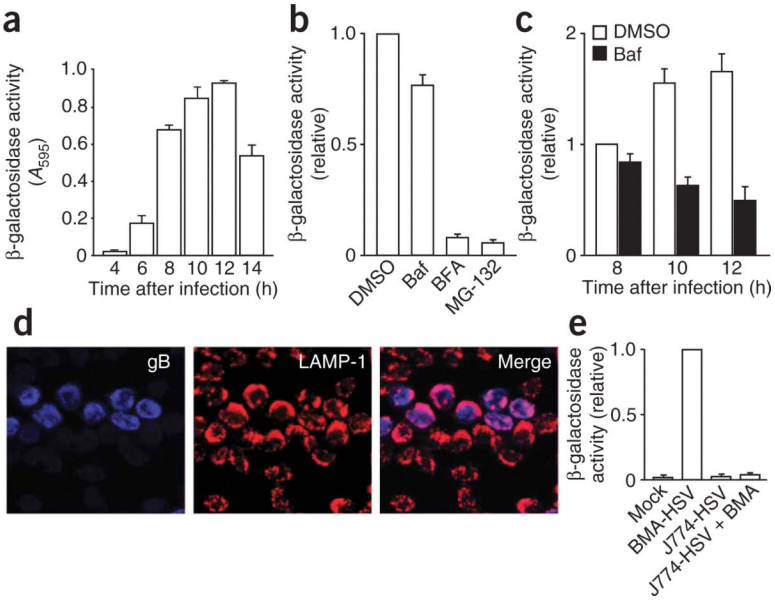

Figure 1.

A vacuolar pathway participates in the processing of endogenous viral proteins for presentation on MHC class I molecules. (**a**) Activation of the gB-specific $CD8^+$ T cell hybridoma (which expresses β-galactosidase as an indicator of T cell activation) by macrophages infected for various times (horizontal axis) with HSV-1, then incubated for 12 h at 37 °C with the hybridoma. A_{595}, absorbance at 595 nm. (**b**) Activation of the hybridoma as described in **a**, with the addition of dimethyl sulfoxide (DMSO; negative control), bafilomycin A (Baf), brefeldin A (BFA) or MG-132 at 2 h after macrophage infection. (**c**) Activation of the hybridoma as described in **a**, with the addition of bafilomycin A at 2 h after macrophage infection. (**d**) Immunofluorescence microscopy of gB (blue) and LAMP-1 (red) in HSV-1-infected macrophages; pink indicates colocalization. Original magnification, ×40. (**e**) $CD8^+$ T cell–stimulatory capacity (as described in **a**) of uninfected macrophages (Mock), of BMA (BMA-HSV) or J774 (J774-HSV) macrophages infected for 8 h with HSV-1, and of cocultures of J774 macrophages ($H\text{-}2^d$) infected for 1 h with HSV-1, then mixed with uninfected BMA ($H\text{-}2^b$) macrophages at a ratio of 1:1 and cultured together for 8 h (J774-HSV + BMA). Results in **b,c,e** are normalized to results obtained for $CD8^+$ T cells stimulated with macrophages treated with DMSO (**b,c**) or infected BMA macrophages (**e**) and are presented in arbitrary units. Data are from one representative of three independent experiments (mean and s.d. of triplicate samples; **a**), are from three independent experiments (mean and s.e.m. of triplicate samples error bars; **b,c,e**) or are representative of three independent experiments (**d**).

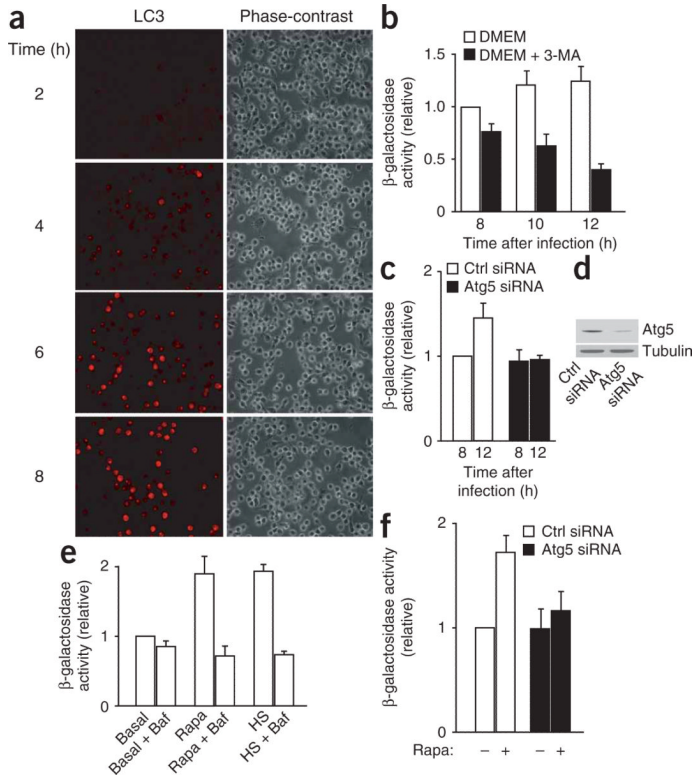

Figure 2.

Autophagy induced during HSV-1 infection contributes to the processing and presentation of endogenous viral antigens on MHC class I molecules. (**a**) Immunofluorescence microscopy of LC3 expression in macrophages infected for 2–8 h (left margin) with HSV-1. Original magnification, ×20. (**b**) Activation of the gB-specific $CD8^+$ T cell hybridoma (described in **Fig. 1a**) by macrophages infected for various times (horizontal axis) with HSV-1, with (DMEM + 3-MA) or without (DMEM) the addition of 3-methyladenine 2 h after infection, then incubated for 12 h at 37 °C with the hybridoma. (**c**) Activation of the hybridoma (as described in **b**) by macrophages transfected for 60 h with control (Ctrl) siRNA or Atg5-specific siRNA, then infected for 8 h or 12 h with HSV-1. (**d**) Immunoblot analysis of Atg-5 in siRNA-treated macrophages. (**e**) Activation of the hybridoma (as described in **b**) by macrophages infected with HSV-1 and incubated at 37 °C (Basal), incubated for 12 h at 39 °C before being infected with HSV-1 (heat shock (HS)), or treated with rapamycin during HSV-1 infection (Rapa), with (+ Baf) or without the addition of bafilmycin A at 2 h after infection. (**f**) Activation of the hybridoma (as described in **b**) by macrophages transfected for 60 h with control siRNA or Atg5-specific siRNA, then infected for 8 h with HSV-1, with (+) or without (–) the addition of rapamycin at 2 h after infection. Results in **b,c,e,f** are normalized to results obtained for $CD8^+$ T cells stimulated with macrophages infected for 8 h at 37 °C without further treatment (**b,e**) or infected macrophages treated with control siRNA (**c,f**) and are presented in arbitrary units. Data are representative of three independent experiments (**a,d**) or are from three independent experiments (mean and s.e.m. of triplicate samples; **b,c,e,f**).

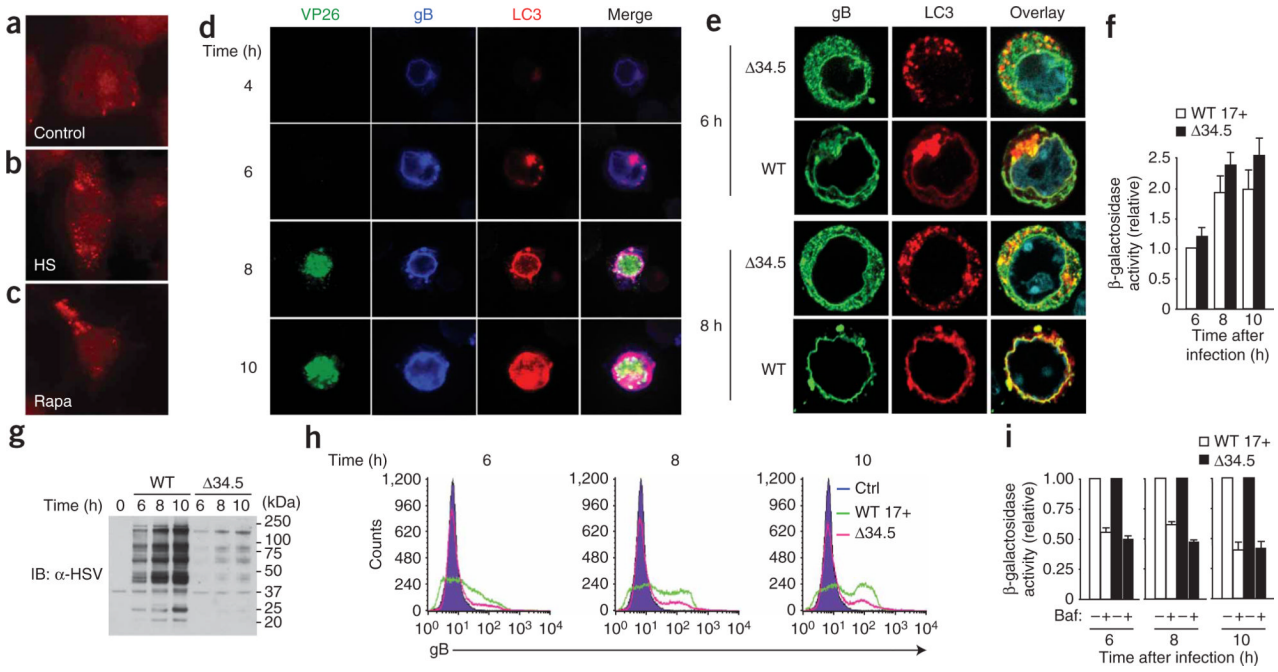

Figure 3.

Both gB and LC3 accumulate in perinuclear regions during HSV-1 infection. (**a–c**) Immunofluorescence microscopy of uninfected macrophages incubated at 37 °C (control; **a**), subjected to mild heat shock (**b**) or treated with rapamycin (**c**), then stained with anti-LC3. (**d**) Immunofluorescence microscopy of the expression of LC3, gB and GFP (VP26) by macrophages infected for various times (left margin) with HSV-1. White indicates colocalization. (**e**) Immunofluorescence microscopy of macrophages infected for 6 h or 8 h (left margin) with wild-type HSV-1 (WT) or HSV-1 lacking ICP34.5 (Δ34.5). Blue, staining of nuclei with DAPI (4,6-diamidino-2-phenylindole). Original magnification, ×100 (**a–c**) or ×63 (**d,e**). Results in **a–e** are representative of three independent experiments. (**f**) Activation of the gB-specific $CD8^+$ T cell hybridoma (as described in **Fig. 1a**) by macrophages infected for various times (horizontal axis) with wild-type HSV-1 strain 17+ (WT 17+) or Δ34.5 HSV-1. Data are from three independent experiments (mean and s.e.m. of triplicate samples). (**g,h**) Immunoblot analysis (IB; **g**) and flow cytometry (**h**) of the expression of HSV-1 proteins (**g**) and gB (**h**) in macrophages infected for various times (above lanes (**g**) or plots (**h**)) with wild-type or Δ34.5 HSV-1. Ctrl, control (uninfected BMA macrophages; **h**). Data are representative of two (**g**) or three (**h**) independent experiments. (**i**) Activation of the gB-specific $CD8^+$ T cell hybridoma (as described in **Fig. 1a**) by macrophages infected for various times (below graph) with wild-type or Δ34.5 HSV-1, with (+) or without (–) the addition of bafilomycin A at 2 h after infection. Results in **f,i** are normalized to results obtained for $CD8^+$ T cells stimulated with macrophages infected for 6 h with wild-type virus (**f**) or with infected macrophages incubated without bafilomycin (**i**) and are presented in arbitrary units. Data are from three independent experiments (mean and s.e.m. of triplicate samples).

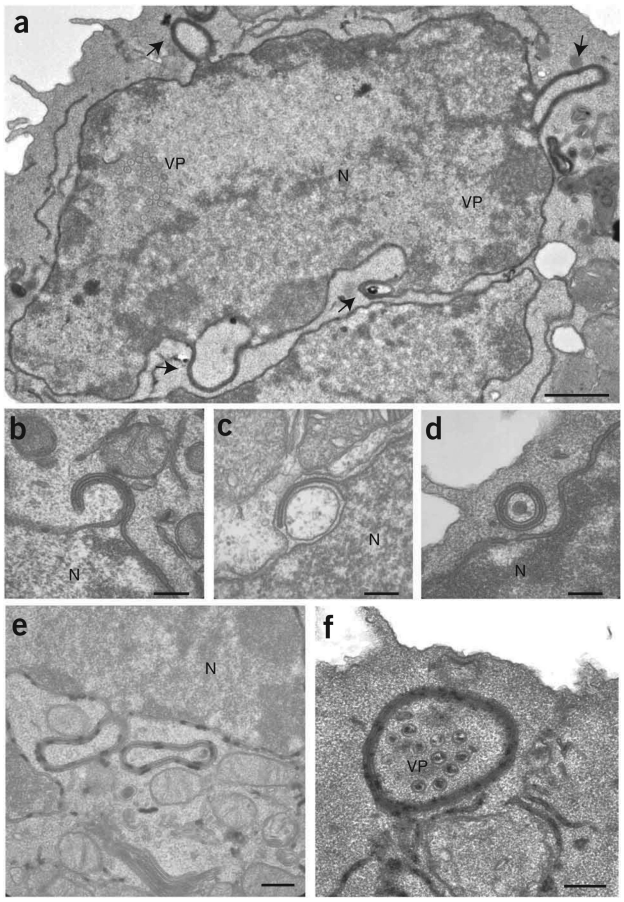

Figure 4.

HSV-1 induces the formation of autophagosome-like structures from the nuclear envelopes of infected macrophages. Electron microscopy of macrophages 10 h after infection with HSV-1. (**a**) Arrows indicate membrane-coiled structures emerging from the nucleus of an infected cell. (**b–d**) Four-layered membrane structures formed by coiling of the nuclear membrane. (**e,f**) Glucose-6-phosphatase (black deposits) on autophagosome-like structures emerging from the nuclear envelope or free in the cytoplasm, and viral capsids in the cytoplasm engulfed in the lumen of an autophagosome-like compartment. N, nucleus; VP, viral particles. Scale bars, 1 μm (**a**), 0.25 μm (**b–d,f**) or 0.4 μm (**e**). Images are representative of three independent experiments with at least 100 cell profiles in each.

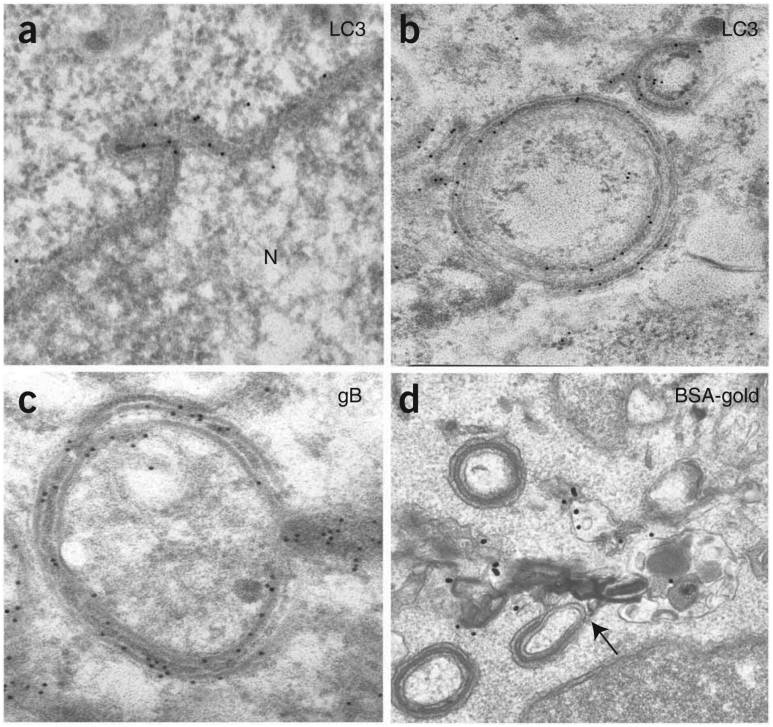

Figure 5.
The four-layered membrane structures that emerge from the nuclear envelope have autophagosome-like features. Immunoelectron microscopy of macrophages 10 h after infection with HSV-1. (**a–c**) Accumulation of LC3 (**a,b**) and gB (**c**). (**d**) Fusion of four-layered membrane structures and lysosomes preloaded with bovine serum albumin–gold (BSA-gold; black dots). Original magnification, ×54,800 (**a,b**), ×69,000 (**c**) or ×38,000 (**d**). Images are representative of three (**a–c**) or two (**d**) independent experiments.

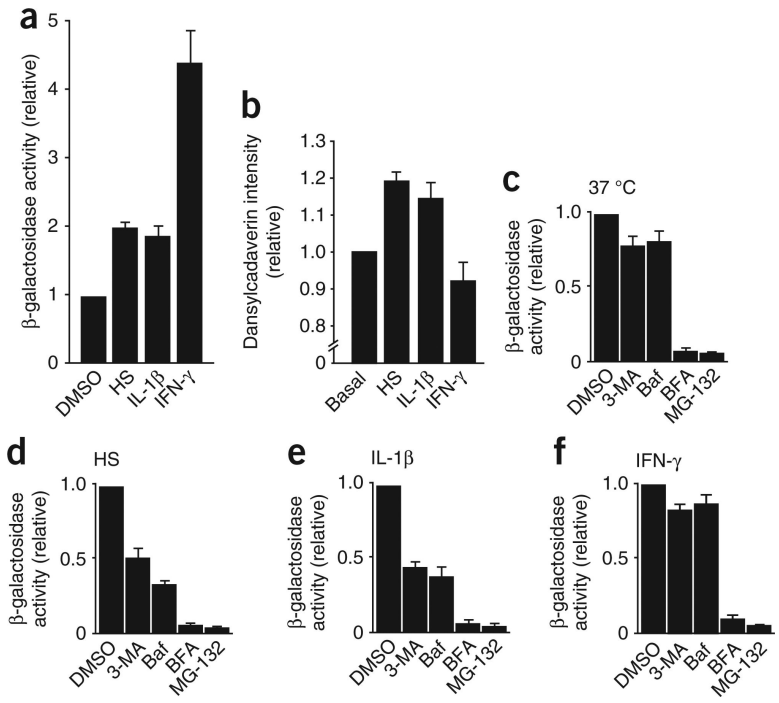

Figure 6.

Involvement of lytic vacuolar compartments in the processing and presentation of endogenous antigens on MHC class I molecules after treatment with proinflammatory cytokines. (**a**) Activation of the gB-specific $CD8^+$ T cell hybridoma (as described in **Fig. 1a**) by macrophages exposed to DMSO (negative control), mild heat shock, IL-1β or IFN-γ. (**b**) Dansylcadaverin staining of untreated macrophages (Basal) or macrophages exposed to mild heat shock, IFN-γ or IL-1β and infected for 8 h with wild-type HSV-1, normalized to the signal obtained in basal conditions and presented in arbitrary units. (**c–f**) Activation of the gB-specific $CD8^+$ T cell hybridoma (as described in **Fig. 1a**) by macrophages incubated at 37 °C (**c**) or exposed to mild heat shock (**d**), IL-1β (**e**) or IFN-γ (**f**) and infected for 8 h with wild-type HSV-1 with the addition of DMSO (negative control), 3-methyladenine, bafilomycin, brefeldin A or MG-132 at 2 h after infection. Results in **a,c–f** are normalized to results obtained for $CD8^+$ T cells stimulated with macrophages incubated with DMSO in each condition and are presented in arbitrary units. Data are from three independent experiments (mean and s.e.m. of triplicate samples).